sors represents an additional dimension of sensitivity and specificity for molecular imaging. The depletion process generating the image contrast depends on several parameters, including saturation power and time, sensor concentration, and ambient temperature. The latter parameter provides another promising approach to increase sensitivity even further, because the exchange rate increases considerably when approaching 37°C (*10*). Characterization of the saturation dynamics is currently under way and will reveal optimized parameters for future applications.

The technique is also quite promising for biomedical imaging in vivo. A typical surface coil of 20 cm diameter detects a volume of ca. 2.1 liters, thus decreasing S/N for a $(2.8\ mm)^3$ voxel by a factor of 27.2 compared with our setup. This loss is less than 50% of the gain for an optimized system using >45% polarized isotopically enriched ^{129}Xe. An isotropic resolution of 2 to 3 mm is feasible without signal averaging for a concentration of pure polarized ^{129}Xe that is ~2 μM in tissue. This minimum value is below those observed for direct injection of Xe-carrying lipid solutions into rat muscle (70 μM) or for inhalation delivery for brain tissue (8 μM) used in previous studies that demonstrated Xe tissue imaging in vivo (*17*). Sensitive molecular imaging of the biosensor is therefore possible as long as the distribution of dissolved xenon can be imaged with sufficient S/N and the biosensor target is not too dilute, because HYPER-CEST is based on the detection of the free Xe resonance, not direct detection of the biosensor resonance.

The HYPER-CEST technique is amenable to any type of MRI image acquisition methodology. We demonstrated CSI here, but faster acquisition techniques that incorporate a frequency encoding domain such as FLASH (fast low angle shot) have been successfully used to acquire in vivo Xe tissue images (*17*).

The modular setup of the biosensor (i.e., the nuclei that are detected are not covalently bound to the targeting molecule) allows accumulation of the biosensor in the tissue for minutes to hours before delivery of the hyperpolarized xenon nuclei, which have much higher diffusivity. In combination with the long spin-lattice relaxation time of Xe, this two-step process optimally preserves the hyperpolarization before signal acquisition. Biosensor cages that yield distinct xenon frequencies allow for multiplexing to detect simultaneously several different targets (*18*). Also the serum- and tissue-specific Xe NMR signals (*19*, *20*) arising after injection of the carrier medium can be used for perfusion studies (Fig. 3B) in living tissue, making Xe-CSI a multimodal imaging technique.

References and Notes

1. J. M. Tyszka, S. E. Fraser, R. E. Jacobs, *Curr. Opin. Biotechnol.* **16**, 93 (2005).
2. A. Y. Louie *et al.*, *Nat. Biotechnol.* **18**, 321 (2000).
3. S. Aime, C. Carrera, D. Delli Castelli, S. Geninatti, E. Terreno, *Angew. Chem. Int. Ed.* **44**, 1813 (2005).
4. M. S. Albert *et al.*, *Nature* **370**, 199 (1994).
5. M. M. Spence *et al.*, *Proc. Natl. Acad. Sci. U.S.A.* **98**, 10654 (2001).
6. T. J. Lowery *et al.*, *Magn. Reson. Imaging* **21**, 1235 (2003).
7. K. Bartik, M. Luhmer, J. P. Dutasta, A. Collet, J. Reisse, *J. Am. Chem. Soc.* **120**, 784 (1998).
8. C. Hilty, T. J. Lowery, D. E. Wemmer, A. Pines, *Angew. Chem. Int. Ed.* **45**, 70 (2006).
9. S.-I. Han *et al.*, *Anal. Chem.* **77**, 4008 (2005).
10. M. M. Spence *et al.*, *J. Am. Chem. Soc.* **126**, 15287 (2004).
11. A. Bifone *et al.*, *Proc. Natl. Acad. Sci. U.S.A.* **93**, 12932 (1996).
12. K. M. Ward, A. H. Aletras, R. S. Balaban, *J. Magn. Res.* **143**, 79 (2000).
13. A. A. Maudsley, S. K. Hilal, W. H. Perman, H. E. Simon, *J. Magn. Res.* **51**, 147 (1983).
14. N. Goffeney, J. W. M. Bulte, J. Duyn, L. H. Bryant, P. C. M. van Zijl, *J. Am. Chem. Soc.* **123**, 8628 (2001).
15. K. Knagge, J. Prange, D. Raftery, *Chem. Phys. Lett.* **397**, 11 (2004).
16. J. L. Mynar, T. J. Lowery, D. E. Wemmer, A. Pines, J. M. Frechet, *J. Am. Chem. Soc.* **128**, 6334 (2006).
17. B. M. Goodson *et al.*, *Proc. Natl. Acad. Sci. U.S.A.* **94**, 14725 (1997).
18. G. Huber *et al.*, *J. Am. Chem. Soc.* **128**, 6239 (2006).
19. J. P. Mugler *et al.*, *Magn. Res. Med.* **37**, 809 (1997).
20. S. D. Swanson, M. S. Rosen, K. P. Coulter, R. C. Welsh, T. E. Chupp, *Magn. Res. Med.* **42**, 1137 (1999).

21. This work was supported by the Director, Office of Science, Office of Basic Energy Sciences, Materials Sciences and Engineering Division, of the U.S. Department of Energy under contract no. DE-AC03-76SF00098. L.S. acknowledges support from the Deutsche Forschungsgemeinschaft (SCHR 995/1-1) through an Emmy Noether Fellowship. T.J.L. acknowledges the Graduate Research and Education in Adaptive bio-Technology (GREAT) Training Program of the UC Systemwide Biotechnology Research and Education Program (no. 2005-264), and C.H. acknowledges support from the Schweizerischer Nationalfonds through a postdoctoral fellowship.

Supporting Online Material
www.sciencemag.org/cgi/content/full/314/5798/446/DC1
Materials and Methods
Fig. S1
References

28 June 2006; accepted 29 August 2006
10.1126/science.1131847

Wetland Sedimentation from Hurricanes Katrina and Rita

R. Eugene Turner,[1,2]* Joseph J. Baustian,[1,2] Erick M. Swenson,[1,2] Jennifer S. Spicer[2]

More than 131 × 10⁶ metric tons (MT) of inorganic sediments accumulated in coastal wetlands when Hurricanes Katrina and Rita crossed the Louisiana coast in 2005, plus another 281 × 10⁶ MT when accumulation was prorated for open water area. The annualized combined amount of inorganic sediments per hurricane equals (i) 12% of the Mississippi River's suspended load, (ii) 5.5 times the inorganic load delivered by overbank flooding before flood protection levees were constructed, and (iii) 227 times the amount introduced by a river diversion built for wetland restoration. The accumulation from hurricanes is sufficient to account for all the inorganic sediments in healthy saltmarsh wetlands.

Inorganic sediments accumulating in coastal wetlands may be delivered from inland sources via (i) unconstrained overbank flooding, (ii) explosive releases through unintentional breaks in constructed levees, and (iii) river diversions. They may also arrive from offshore during tidal inundation or storm events. It is important to know the quantities delivered by each pathway to understand how inorganic sediments contribute to wetland stability and to spend wetland restoration funds effectively. Here we estimate the amount of inorganic sediments deposited on wetlands of the microtidal Louisiana coast during Hurricanes Katrina and Rita.

Hurricanes Katrina and Rita passed through the Louisiana (LA) coast on 29 August and 24 September, 2005, respectively, leaving behind a devastated urban and rural landscape. Massive amounts of water, salt, and sediments were redistributed across the coastal zone within a few hours as a storm surge of up to 5 m propagated in a northerly direction at the coastline south of New Orleans, LA (Katrina), and near Sabine Pass, Texas (TX) (Rita), inundating coastal wetlands in the region. A thick deposit of mud remained in these coastal wetlands after the storm waters receded (Fig. 1). We used this post-storm remnant to learn about how coastal systems work.

The loss of LA's coastal wetlands peaked between 1955 and 1978 at 11,114 ha $year^{-1}$ (*1*) and declined to 2591 ha $year^{-1}$ from 1990 to 2000 (*2*). Coastal wetlands, barrier islands, and shallow waters are thought to provide some protection from hurricanes, by increasing resistance to storm surge propagation and by lowering hurricane storm surge height (*3*). Restoring LA's wetlands has become a political priority, in part because of this perceived wetland/storm surge connection. A major part of LA's restoration effort is to divert part of the Mississippi River into wetlands, and at considerable cost [ref. (*S1*) in supporting online material (SOM)]. Widely adopted assumptions supporting this

[1]Coastal Ecology Institute, [2]Department of Oceanography and Coastal Sciences, Louisiana State University, Baton Rouge, LA 70803, USA.

*To whom correspondence should be addressed. E-mail: euturne@lsu.edu

diversion are that flood protection levees have eliminated overbank flooding, which has caused diminished sediment accumulation and eventual wetland loss, and introducing sediments into estuaries via river diversions will enhance wetland restoration.

If increasing inorganic sediment loading to coastal wetlands is important for their restoration, then it is important to quantify the major sediment pathways. Hurricanes Katrina and Rita obviously brought some inorganic sediment into the coastal wetlands, but how much, and where was it distributed? A few measurements of the inorganic sediments accumulating from a hurricane have been made at specific sites along the coast (*4–8*) [ref. (*S7*) in SOM], but until this study there were no coastwide data on the inorganic sediments accumulating from hurricanes. Here we show that the dominant pathway of inorganic sediments into the microtidal LA coastal wetlands is from offshore to inshore during hurricanes, and not from overbank flooding along the main channel of the Mississippi River, from smaller storm events, or from tidal inundations.

We sampled from the shoreline to the onshore limit of storm sediment deposition in wetlands (*9*) (Fig. 1A). We collected samples from all coastal watersheds in LA and at seven sites in eastern TX, using a helicopter and airboat (145 samples) or by walking out >20 m into the wetland from access points reached by boat or car (53 samples). Freshly deposited mud was easily identifiable from the layers beneath on the basis of color, texture, and density, and by the absence of plant debris (Fig. 1E). At least one preliminary sampling was done at each location (often three or four) before the final sample was taken. Samples for sediment depth (in centimeters) and density (in grams per cm^3) were taken only over the vegetation zone and not in rivulets between clumps of wetland plants.

The average bulk density of the newly deposited material was 0.37 g cm^{-3} (±1 SD = ± 0.35; range, 0 to 1.78 g cm^{-3}; n = 170 samples); it was highest near the coastline and decreased inland (Fig. 2B). The bulk density of material in these wetlands was determined by the amount of inorganic materials, not the organic content, and so bulk density multiplied by deposition height is an estimate of inorganic sediment deposition (*9*, *10*). Sediment with a bulk density >1 was largely composed of sand (Fig. 1A) (*9*). There was sparse plant debris (stems, leaves, and roots) in the newly deposited sediments within a few kilometers from the shoreline. The unconfirmed hypothesis is that the source materials from offshore came from where the bottom resistance to the hurricane winds before landfall was the greatest: in the shallow water zone immediately offshore of the deposition site.

The average dry weight accumulation of the deposition layer at all sampled locations was 2.23 g cm^{-2} (±1 SD = ± 3.4; range, 0 to 28.6 g cm^{-2}; n = 169) and 2.25 g cm^{-2} in the deltaic plain. The thickness of the newly deposited mud was 5.18 cm (±1 SD = ± 7.7; range, 0 to 68 g cm; n = 186). The thickest newly deposited sediments were observed inland of the area of maximum bulk density in eastern LA but were coincidental with the sediments of highest bulk density in western LA (Fig. 2C). The annualized average sediment accumulation from one hurricane was 89% of the average accumulation in healthy saltmarsh wetlands in the deltaic plain [0.166 g cm^{-2} $year^{-1}$ (*10*)].

Sediment deposition (in grams per cm^2) was greatest near the center of the storm track (Fig. 2D). The highest values in the Chenier Plain were on the east side of the hurricane path, where counterclockwise winds brought a storm surge inland, and were least on the western side, where water was withdrawn in a southerly direction out of the wetlands (Fig. 2, D to F). The greatest deposition in the Deltatic Plain was in the Breton Sound estuary, on the east side of the Mississippi River. The marshes within the 4° longitude distance between the two hurricanes (approximately 300 km) had intermediate rates of deposition. The peak water level, but not sediment accumulation, was higher in western Lake Pontchartrain during Hurricane Rita than during Hurricane Katrina because of these differences in wind fields (*11*). The peak in bulk density was highest on the eastern side of the center of the storm track.

There were peaks in sediment deposition where navigation channels confined the incoming storm surge to a narrow area at Sabine Pass, TX, and in the industrial canal by Paris Road, New Orleans, where the Intracoastal Waterway

Fig. 1. Examples of sediments deposited by Hurricanes Katrina and Rita. (**A**) Sand overwash on the former location of the coastal community of Holly Beach, LA (photo taken 18 November 2005 by R.E.T.). (**B**) Mud on the lawn of a St. Bernard Parish subdivision home (photo taken 27 September 2005 by M. Collins). (**C**) Mud on the marsh surface brought by Hurricanes Katrina and Rita (photo taken 16 November 2005 by J.B.). (**D**) Recent mud deposit (10.5 cm) accumulated over a root mass in the St. Bernard estuary (photo taken 16 November 2005 by J.B.). (**E**) Dried mud on the lawn of a Chalmette, LA, subdivision home, September 2005 (photo taken by R. Richards).

meets the Mississippi River Gulf Outlet. These observations are consistent with results from modeled storm surge velocities (*12*).

The total amount of recently deposited wetland sediments on the LA coast was calculated using information on the average sediment accretion and wetland area for each of four to six subunits of four coastal regions. The minimum amount of inorganic sediment brought in by these two hurricanes was estimated to be 131×10^6 metric tons (MT) (*9*) (Table 1). The average occurrence of a Category 3 or larger hurricane on this coast was every 7.88 years from 1879 to 2005 (*9*) (table S1). The annualized deposition from one hurricane would be 8.3×10^6 MT year^{-1} if all hurricanes brought an equal amount of sediments to these wetlands. If sediments from these hurricanes are deposited in open-water areas at the same rate as in wetlands (*9*), then the pro rata deposition for open-water areas is proportional to the open water/wetland area (*1*) and is equal to 17.8×10^6 MT year^{-1}, for a combined sediment deposition of 26.1×10^6 MT year^{-1}.

The sediment accumulations in wetlands and open water were 4.0 and 8.5%, respectively, of the average annual suspended sediment load of the Mississippi River (210×10^6 MT year^{-1}) (Table 1) (*13*). The more frequent smaller storms not included in this analysis may also transport substantial amounts of inorganic material (*14*, *15*).

The amount of sediments delivered to coastal wetlands by Hurricanes Katrina and Rita was greater than the estimated amounts once flowing through or over Mississippi River banks. The suspended sediments overflowing unconfined (natural) levees of the Mississippi River in the past century were 4.8×10^6 MT year^{-1}, and 1.7×10^6 MT year^{-1} in a confined levee system with occasional crevasses (Table 1). The Caernarvon Diversion, a restoration project located downstream from New Orleans, LA, delivered a 2-year average sediment load of 0.115×10^6 MT year^{-1} (*16*). One conclusion to be drawn from these numbers is that the amount of sediment deposited on these wetlands from an average Category 3 or larger hurricane is 1.7 times the amount potentially available through unconfined overbank flooding, 4.6 times more than through crevasses in the unconfined channel, and 72 times more than from this river diversion. The combined sediment accumulation in wetlands and open water resulting from an average Category 3 or larger hurricane is 5.5 times larger than the material delivered by unconfined flow in the Mississippi River and 227 times larger than that delivered by the Caernarvon Diversion.

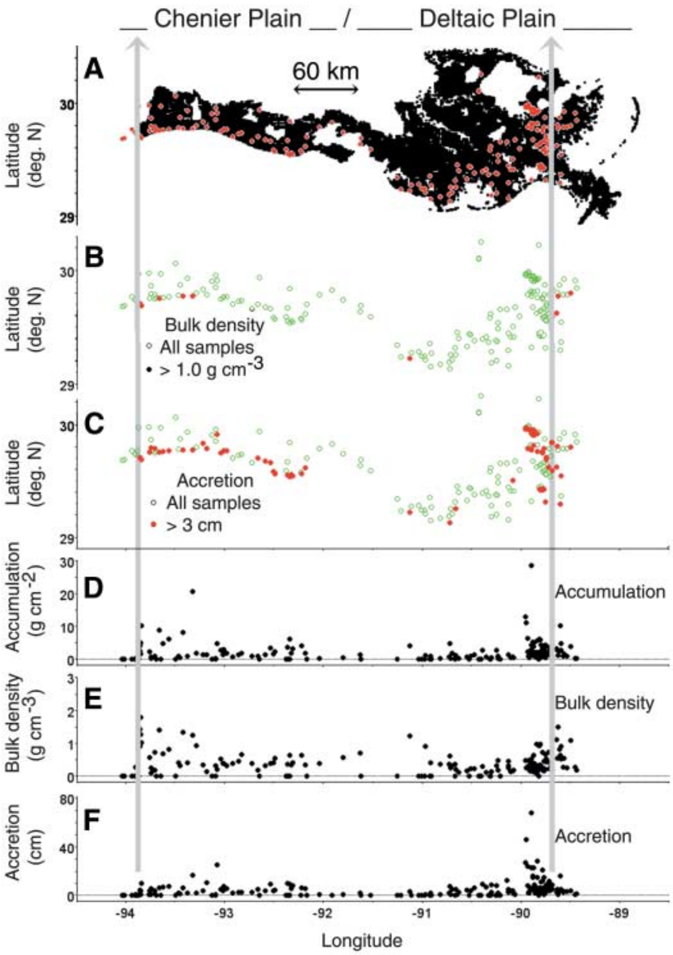

Fig. 2. Location of recent sediment samples and data arranged by longitude. (**A**) Sample locations (red dots) and the distribution of coastal wetlands in southern LA (black background). The vertical gray arrow is the crossing location of Hurricanes Rita (western LA) and Katrina (eastern LA). (**B**) All samples (open circles) and samples with a bulk density value >1.0 g cm^{-3} (red dots). (**C**) All samples (open circles) and samples with a vertical accretion >3 cm (red dots). (**D**) Accumulation relative to the longitude of sample collection (black circles). (**E**) Bulk density relative to the longitude of sample collection. (**F**) Vertical accretion relative to the longitude of sample collection.

However, these comparisons are conservative estimates. Not all of the inorganic sediment flowing from rivers and over or through levees is deposited onto a wetland. Levees are higher than the surrounding land because inorganics settle out onto the levees or within the nearby marshes. Also, the peak in river heights, and hence in discharge, occurs in the spring when water levels in the estuary are at their seasonal low and wetlands are infrequently flooded (*17*). Sediments that do accumulate are deposited close to the diversion. For example, the Caernarvon Diversion distributes about 50% of its sediments into the wetlands for a maximum distance of about 6 km, covering about 15% of a direct path to the coastline (Table 1) (*18*). Hurricanes, in contrast, are much more democratic in that they flood the entire coastal landscape with new sediments.

A coastwide perspective on sediment loading to these wetlands, and perhaps to other microtidal coastal wetlands, is that most of the inorganics accumulating in them went down the Mississippi's birdfoot delta before they were deposited during large storms. The estimates indicate that the amount of storm-transported material is much greater than that introduced to wetlands from the historical overbank flow, from crevasses, or from river diversions. In particular, hurricanes appear to be the overwhelming pathway for depositing new inorganic sediments in coastal wetlands in western LA, because the few riverine sources bring relatively trivial amounts of inorganic sedi-

Table 1. Estimates of the sediment source pathways for the Mississippi River deltaic plain in Louisiana.

Sediment source pathways	Amount (10^6 MT year^{-1})
Mississippi River discharge into ocean (*13*)	210
One hurricane every 7.88 years (table S1)	
Onto wetland only	8.3
Onto wetland and into open water (*9*)	25.9
Overbank flooding (before flood protection levees) and into open water (*22*)	4.79
Crevasses through levees and into open water (*22*)	1.81
Caernarvon Diversion	
Into the estuary (*16*)	0.115
Onto wetland (*18*)	0.06

ments into the marsh. Because hurricanes are so important to the inorganic sediment budget, other factors must be considered to understand how to reduce wetland losses and further their restoration. Changes in the in situ accumulation of organics, rather than the reduction of inorganic sediments arriving via overbank flooding, are implicated as a causal agent of wetland losses on this coast. This is illustrated by the fact that the soil volume occupied by organic sediments plus water in healthy saltmarsh wetlands is >90% (*10*) and is certainly the same or higher in wetlands of lower salinity. This organic portion plays a major role in wetland soil stability and hence in wetland ecosystem health (*19*).

References and Notes

1. R. H. Baumann, R. E. Turner, *Environ. Geol. Water Res.* **15**, 189 (1990).
2. T. A. Morton, J. C. Bernier, J. A. Barras, N. F. Ferina, *USGS Open-File Rep.* 2005-1215 (2005).
3. G. W. Stone, X. Zhang, A. Sheremet, *J. Coastal Res.* **44**, 40 (2005).
4. J. M. Rybczyk, D. R. Cahoon, *Estuaries* **25**, 985 (2002).
5. M. L. Parsons, *J. Coastal Res.* **14**, 939 (1998).
6. D. R. Cahoon *et al.*, *J. Coastal Res.* **21** (special issue), 280 (1995).
7. J. P. Morgan, L. G. Nichols, M. Wright, *Morphological Effect of Hurricane Audrey on the Louisiana Coast* (contribution no. 58-3, Coastal Studies Institute, Louisiana State Univ., Baton Rouge, LA, 1958).
8. J. A. Nyman, R. D. DeLaune, H. H. Roberts, W. H. Patrick Jr., *Mar. Ecol. Prog. Ser.* **96**, 269 (1992).
9. Materials and methods are available as supporting material on *Science* Online.
10. R. E. Turner, E. M. Swenson, C. S. Milan, in *Concepts and Controversies in Tidal Marsh Ecology*, M. Weinstein, D. A. Kreeger, Eds. (Kluwer, Dordrecht, Netherlands, 2001), pp. 583–595.
11. The peak water measured by U.S. Geological Survey water-level gage 30174809020900, at Pass Manchac Turtle Cove near Ponchatoula, LA, in the western Lake Pontchartrain watershed, was about 6 cm higher during Hurricane Rita than during Hurricane Katrina, even though the hurricane path was over 300 km further away.
12. Storm surge model results for Hurricanes Katrina and Rita are available at the Louisiana State University Hurricane Center Web sites (http://hurricane.lsu.edu/floodprediction/katrina/deadly_funnel1.jpg and http://hurricane.lsu.edu/floodprediction/rita24/images/adv24_SurgeTX_LA.jpg).
13. G. J. Chakrapani, *Curr. Sci.* **88**, 569 (2005).
14. R. H. Baumann, thesis, Louisiana State Univ., Baton Rouge, LA (1980).
15. D. J. Reed, N. De Luca, A. L. Foote, *Estuaries* **20**, 301 (1997).
16. G. A. Snedden, J. E. Cable, C. Swarzenski, E. Swenson, *Estuar. Coastal Shelf Sci.,* in press.
17. R. E. Turner, *Estuaries* **14**, 139 (1991).
18. K. W. Wheelock, thesis, Louisiana State Univ., Baton Rouge, LA (2003).
19. R. E. Turner, E. M. Swenson, C. S. Milan, J. M. Lee, T. A. Oswald, *Ecol. Res.* **19**, 29 (2004).
20. R. H. Kesel, *Environ. Geol. Water Res.* **11**, 271 (1988).
21. C. M. Belt Jr., *Science* **189**, 681 (1975).
22. Kesel (*20*) estimated the sediment load in the spring floods using water records from 1950 to 1983 and determined the amount of sediment that would be available from unconfined overbank flooding if the levees were not there. The estimate is actually an overestimate of the amount available, because the artificial constriction of the river channel throughout the basin raised the flood stage for the same-sized discharge event (*21*).

23. Supported by the NSF Division of Geomorphology and Land-Use Dynamics (award EAR-061250), the National Oceanic and Atmospheric Administration Coastal Ocean Program MULTISTRESS (award no. NA16OP2670), and a Louisiana Board of Regents Fellowship (J.S.S.). We thank J. Gore for assistance in sampling from an airboat; E. Babin for assistance in finding photographs; H. Hampp, our deft, safe, and considerate helicopter pilot; and B. Sen Gupta, N. N. Rabalais, and three anonymous reviewers for constructive reviews of the manuscript.

Supporting Online Material
www.sciencemag.org/cgi/content/full/1129116/DC1
Materials and Methods
SOM Text
Fig. S1
Table S1
References and Notes

24 April 2006; accepted 1 September 2006
Published online 21 September 2006;
10.1126/science.1129116
Include this information when citing this paper.

A Combined Mitigation/Geoengineering Approach to Climate Stabilization

T. M. L. Wigley

Projected anthropogenic warming and increases in CO_2 concentration present a twofold threat, both from climate changes and from CO_2 directly through increasing the acidity of the oceans. Future climate change may be reduced through mitigation (reductions in greenhouse gas emissions) or through geoengineering. Most geoengineering approaches, however, do not address the problem of increasing ocean acidity. A combined mitigation/geoengineering strategy could remove this deficiency. Here we consider the deliberate injection of sulfate aerosol precursors into the stratosphere. This action could substantially offset future warming and provide additional time to reduce human dependence on fossil fuels and stabilize CO_2 concentrations cost-effectively at an acceptable level.

In the absence of policies to reduce the magnitude of future climate change, the globe is expected to warm by ~1° to 6°C over the 21st century (*1*, *2*). Estimated CO_2 concentrations in 2100 lie in the range from 540 to 970 parts per million, which is sufficient to cause substantial increases in ocean acidity (*3*–*6*). Mitigation directed toward stabilizing CO_2 concentrations (*7*) addresses both problems but presents considerable economic and technological challenges (*8*, *9*). Geoengineering (*10*–*17*) could help reduce the future extent of climate change due to warming but does not address the problem of ocean acidity. Mitigation is therefore necessary, but geoengineering could provide additional time to address the economic and technological challenges faced by a mitigation-only approach.

National Center for Atmospheric Research, Post Office Box 3000, Boulder, CO 80307–3000, USA. E-mail: wigley@ucar.edu

The geoengineering strategy examined here is the injection of aerosol or aerosol precursors [such as sulfur dioxide (SO_2)] into the stratosphere to provide a negative forcing of the climate system and consequently offset part of the positive forcing due to increasing greenhouse gas concentrations (*18*). Volcanic eruptions provide ideal experiments that can be used to assess the effects of large anthropogenic emissions of SO_2 on stratospheric aerosols and climate. We know, for example, that the Mount Pinatubo eruption [June 1991 (*19*, *20*)] caused detectable short-term cooling (*19*–*21*) but did not seriously disrupt the climate system. Deliberately adding aerosols or aerosol precursors to the stratosphere, so that the loading is similar to the maximum loading from the Mount Pinatubo eruption, should therefore present minimal climate risks.

Increased sulfate aerosol loading of the stratosphere may present other risks, such as through its influence on stratospheric ozone. This particular risk, however, is likely to be small. The effect of sulfate aerosols depends on the chlorine loading (*22*–*24*). With current elevated chlorine loadings, ozone loss would be enhanced. This result would delay the recovery of stratospheric ozone slightly but only until anthropogenic chlorine loadings returned to levels of the 1980s (which are expected to be reached by the late 2040s).

Figure 1 shows the projected effect of multiple sequential eruptions of Mount Pinatubo every year, every 2 years, and every 4 years. The Pinatubo eruption–associated forcing that was used had a peak annual mean value of –2.97 W/m^2 (*20*, *21*). The climate simulations were carried out using an upwelling-diffusion energy balance model [Model for the Assessment of Greenhouse gas–Induced Climate Change (MAGICC) (*2*, *25*, *26*)] with a chosen climate sensitivity of 3°C equilibrium warming for a CO_2 doubling (2 × CO_2). Figure 1 suggests that a sustained stratospheric forcing of ~–3 W/m^2 (the average asymptotic forcing for the biennial eruption case) would be sufficient to offset much of the anthropogenic warming expected over the next century. Figure 1 also shows how rapidly the aerosol-induced cooling disappears once the injection of material into the stratosphere stops, as might become necessary should unexpected environmental damages arise.

Three cases are considered to illustrate possible options for the timing and duration of aerosol injections. In each case, the loading of the stratosphere begins in 2010 and increases linearly to